ELSEVIER

Journal of Alloys and Compounds 452 (2008) 54–60

Journal of ALLOYS AND COMPOUNDS

www.elsevier.com/locate/jallcom

Thermal conductivities of (U, Pu, Am)O_2 solid solutions

Kyoichi Morimoto [a,*], Masato Kato [a], Masahiro Ogasawara [b], Motoaki Kashimura [a], Tomoyuki Abe [a]

[a] *Japan Atomic Energy Agency, 4-33 Muramatsu, Tokai-mura, Naka-gun, Ibaraki 319-1194, Japan*
[b] *Inspection Development Company, 4-33 Muramatsu, Tokai-mura, Naka-gun, Ibaraki 319-1194, Japan*

Received 18 September 2006; received in revised form 15 December 2006; accepted 21 December 2006
Available online 16 February 2007

Abstract

The thermal conductivities of $(U_{0.7-z}Pu_{0.3}Am_z)O_2$ solid solutions ($z = 0.007$–0.03) were studied by the laser flash method at temperatures from 900 to 1773 K. First, the thermal conductivities of $(U_{0.68}Pu_{0.3}Am_{0.02})O_2$ solid solutions were measured as a function of density ($\rho = 85$–95% of theoretical density). The dependence of the thermal conductivities on the effective porosity $(1 - \rho)$ was evaluated by the correction equations of Loeb, Maxwell–Eucken and Shultz, and then the experimental values were best-fitted with the correction coefficient of $\beta = 0.5$ in the Maxwell–Eucken equation.

The thermal conductivities of $(U_{0.7-z}Pu_{0.3}Am_z)O_2$ solid solutions were found to decrease slightly with increasing Am-content. The thermal conductivities satisfied the classical phonon transport model, $\lambda = (A + BT)^{-1}$ up to about 1500 K. The coefficient A increased linearly with increasing Am-content, and little variation was observed in the coefficient B.

The dependencies of the coefficients A and B on the Am-content were evaluated by the phonon scattering model. The coefficients obtained in the experiment could be theoretically well explained, assuming that the chemical formula of Am-MOX was $U_{(0.7-2z)}{}^{4+}U_z{}^{5+}Pu_{0.3}{}^{4+}Am_z{}^{3+}O_2{}^{2-}$.
© 2007 Elsevier B.V. All rights reserved.

Keywords: Actinide alloys and compounds; Ceramics; Thermodynamic properties

1. Introduction

Thermal conductivity is one of the important thermal physical properties for design and performance analyses of nuclear fuels and many reviews [1,2] and studies [3–12] have been carried out on the thermal conductivities of uranium dioxide (UO_2) and uranium–plutonium mixed oxide (MOX) fuels.

When recycling of MOX fuel is repeated in a fast breeder reactor (FBR), it contains a considerable amount of ^{241}Pu, which has a half life of 14.4 years. Consequently, its daughter nuclide ^{241}Am accumulates in the MOX fuel with time. If the storage time between reprocessing of the irradiated fuel and MOX fuel loading into the reactor becomes long, a considerable amount of ^{241}Am accumulates in the MOX fuel and affects its thermal and mechanical properties. However, there have been no publications on the effects of Am-content on the thermal conductivity of MOX fuel until now.

In this study, three kinds of MOX fuels containing different Am-contents were fabricated, and their thermal conductivities were measured. From these results, the effects of Am-content and density on the thermal conductivity were clarified. In addition, these results were discussed from the viewpoint of phonon scattering.

2. Experimental

2.1. Preparation of specimens

The specimens in this study were UO_2 pellets and three kinds of (U, Pu, Am)O_2 (Am-MOX) pellets. The content of plutonium was about 30% of the total metal content, those of americium were about 0.7, 2.2, and 3.1%. In the following, these Am-MOX pellets of different Am-contents are denoted as 0.7%Am-MOX, 2%Am-MOX, and 3%Am-MOX, respectively. It is known that if plutonium dioxide (PuO_2) is stored for a long period, considerable amounts of ^{241}Am can be taken up. In this study, PuO_2 powders containing 10.7, 7.9 and 2.1 wt% ^{241}Am were used as starting raw powders.

UO_2 and three kinds of Am-MOX specimens were fabricated by conventional powder technology. UO_2 and Am-PuO_2 powders were mixed by mechanical blending in a ball mill for 0.7% and 2%Am-MOX specimens, and by hand blending in a mortar for 3%Am-MOX specimens because the powder

* Corresponding author. Tel.: +81 29 282 1111; fax: +81 29 282 9473.
E-mail address: morimoto.kyoichi@jaea.go.jp (K. Morimoto).

0925-8388/$ – see front matter © 2007 Elsevier B.V. All rights reserved.
doi:10.1016/j.jallcom.2006.12.159

Table 1
Impurity analysis results of the pellets of 0.7%Am-MOX, 2%Am-MOX, UO_2 and the raw material of 3%Am-MOX

Element	0.7%Am-MOX pellet (ppm)	2%Am-MOX pellet (ppm)	UO_2 pellet (ppm)	3%Am-MOX	
				Raw material of PuO_2 (ppm)	Raw material of UO_2 (ppm)
Ag	<5	<5		<5	<0.2
Al	<100	<100	60	135	<10
B	<5	<5	<0.3	<5	<0.3
Cd	<5	<5	<0.6	<5	<0.6
Cr	<50	<50	<10	<50	<10
Cu	<10	<10		<10	<1
Fe	<100	<100	<10	<100	<10
Mg	<15	<15	<2	<15	<2
Mn	<20	<20		<20	<6
Ni	<50	<50	<10	<50	<10
Si	<100	<100		<100	<10
V	<50	<50	<10	<50	<10
Zn	<100	<100		<100	<50
Ca	<30	<30	<10	55	<10
Pb	<30	<30		<30	<10
Sn	<30	<30		<30	<10
Mo	<50	<50		<50	<10
Na	<50	80			<10
Ag + Mn + Mo + Pb + Sn			36.2		
Cu + Si + Ti + Zn			201		

Table 2
Main characteristics of the specimens analyzed

Specimen	0.7%Am-MOX	2%Am-MOX	3%Am-MOX	UO_2
Pu/(U + Pu + Am) (mol%)	29.84	29.52	29.45	
Am/(U + Pu + Am) (mol%)	0.68	2.19	3.09	
Theoretical density (%TD)	91.2–91.5	84.3–95.2	91.4–92.8	92.0–92.8
Specimen weight (g)	0.268–0.288	0.258–0.283	0.245–0.272	0.261–0.270
Diameter (mm)	5.69–5.79	5.46–5.71	5.55–5.58	5.39
Thickness (mm)	1.03–1.07	1.02–1.15	1.02–1.12	1.13

amounts were not so large. The powder was cold-pressed at 4.5 t/cm^2, and the compact was sintered at 1973 K for 3 h under an atmosphere of Ar–5%H_2 mixed gas containing moisture. The dependence of density on the thermal conductivity was studied in 2%Am-MOX. The densities of 2%Am-MOX specimens were adjusted by changing the amount of the two kinds of organic additives, zinc stearate and avicel. The sintered pellets were sliced by a diamond wheel cutter into thin disks about 1 mm thick. The oxygen-to-metal ratios (O/M ratios) of UO_2 specimens were adjusted to 2.00 by heating them at 1973 K for 4 h under an atmosphere of Ar–5%H_2 mixed gas. This mixed gas did not contain moisture. The O/M ratios of the Am-MOX specimens were adjusted to 2.00 by heating them at 1123 K for 5 h under an atmosphere of Ar–5%H_2 mixed gas containing a suitable amount of moisture. The amount of moisture was controlled in order that the oxygen potential ΔG_{O_2} of the atmosphere was −420 kJ/mol at 1123 K, which lies in the range of oxygen potential required to obtain stoichiometric $(U_{0.7}Pu_{0.3})O_2$ mixed oxide [13,14].

The main impurities of 0.7%Am-MOX and 2%Am-MOX pellets are shown in Table 1. The impurities of 3%Am-MOX pellets were not analyzed because of their small amounts; instead, the main impurities of the raw material are shown in Table 1. The densities of specimens measured by an immersion method and some other details of the fabricated specimens are listed in Table 2. The fabricated pellets with O/M ratio of 2.00 were crushed to powders and these powders were measured with an X-ray diffractometer (RINT-1100, Rigaku Co. Ltd.). The diffraction patterns of 0.7%Am-MOX, 2%Am-MOX and 3%Am-MOX showed that each specimen consisted of a single phase with face-centered cubic structure. The lattice parameters of Am-MOX pellets are shown in Fig. 1 and are in good agreement with Vegard's law [15]. From these facts, it was confirmed that the O/M ratio of these specimens was 2.00.

Some 2%Am-MOX specimens were cold-mounted in araldite and polished to a mirror surface. Their ceramographs were observed with a metallurgical microscope (Union Optical Co. Ltd.) for the pore distribution analysis. The ceramography results obtained on the cross sections of two typical specimens (Fig. 2) showed that the pores were dispersed uniformly.

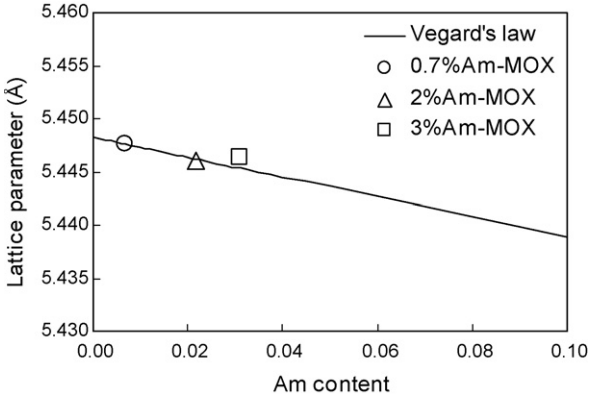

Fig. 1. Lattice parameter of near-stoichiometric 0.7, 2 and 3%Am-MOX as a function of the Am content. Marks are the experimental values. Solid lines are for the lattice parameter of the $(U_{0.7-z}, Pu_{0.3}, Am_z)O_{2.00}$ solid solution calculated from Vegard's law.

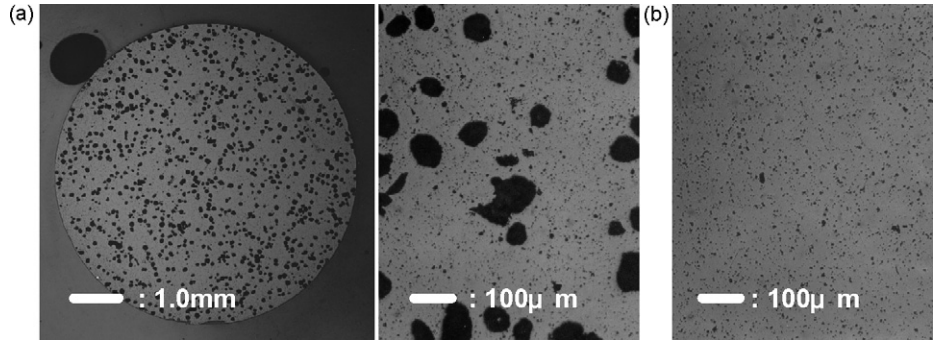

Fig. 2. Ceramographs of typical specimens with different density: (a) specimen with density of 87.3% of theoretical density (TD); (b) specimen with density of 94.8%TD.

The elemental distributions of the above pellets on the mirror-finished surface were analyzed with an electron probe microanalyzer (EPMA/JXA-8800, JEOL Ltd.). Fig. 3 shows the EPMA mapping results obtained on transverse cross sections of 0.7%Am-MOX, 2%Am-MOX and 3%Am-MOX specimens. The 0.7%Am-MOX and 2%Am-MOX specimens had a high degree of homogeneity, and there was no segregation among the constituent elements. Some segregation of uranium was observed in 3%Am-MOX because of its preparation by hand blending, but the amount of segregation was so small that there was no influence on the thermal diffusivity measurements.

2.2. Thermal diffusivity measurements

The thermal diffusivities of specimens were measured at temperatures from 900 to 1773 K with a laser flash apparatus (TC-7000UVH, ULVAC-RIKO Co. Ltd.). The laser was a neodymium glass laser, and its energy per pulse duration of ~0.5 ms was about 17 J. Each specimen was heated in an electric resistance furnace and its temperature was measured with a W–5%Re/W–26%Re thermocouple. The temperature change on the back surface of the specimen, in response to the laser pulse irradiation, was measured with an In–Sb infrared detector at furnace temperatures below 1673 K and with a Si infrared detector at furnace

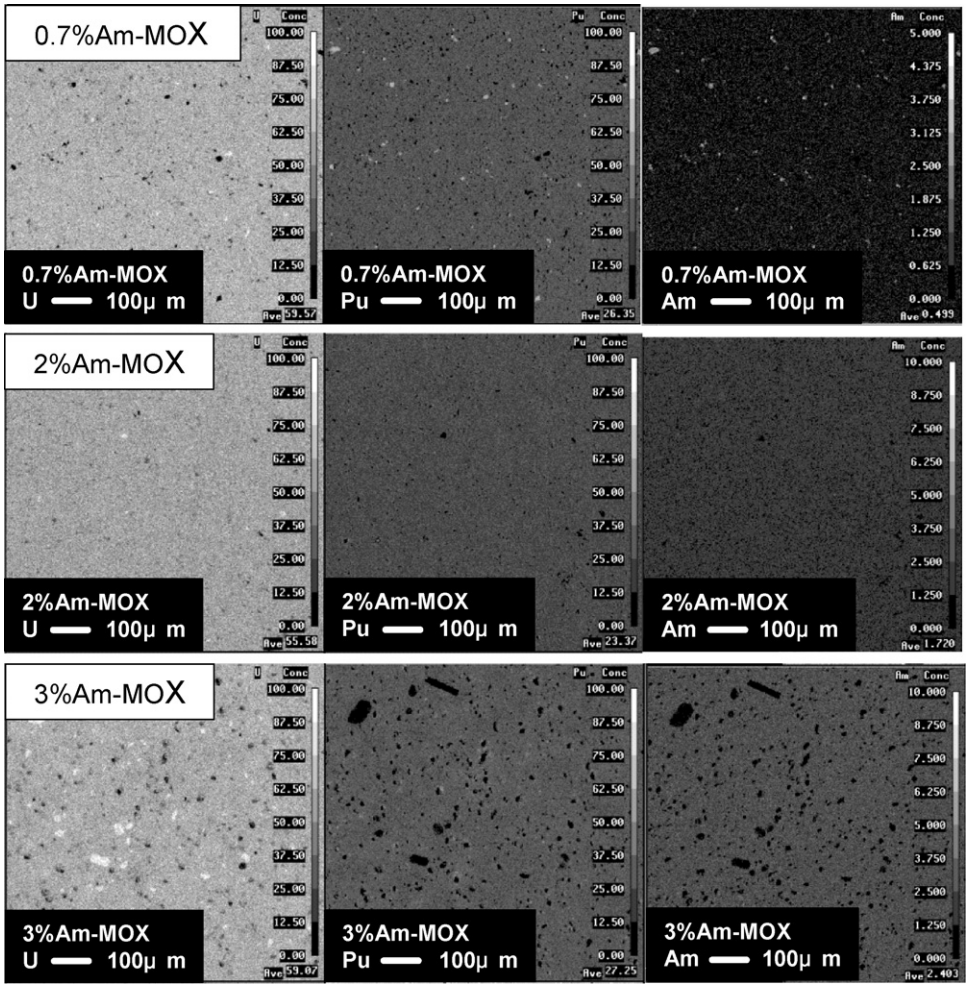

Fig. 3. Electron probe microanalysis mapping results of the Am-MOX.

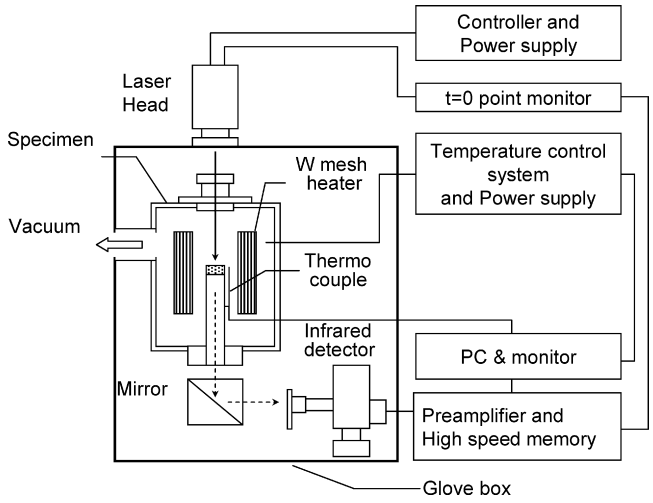

Fig. 4. Schematic diagram of experimental set-up for thermal diffusivity measurements.

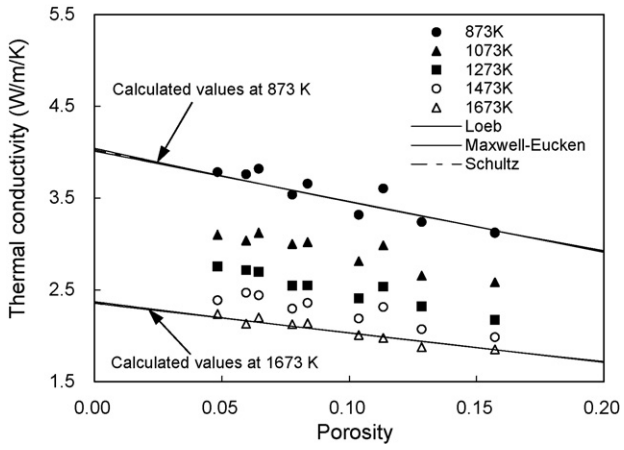

Fig. 5. Thermal conductivities of near-stoichiometric 2%Am-MOX as a function of porosity. Open and solid marks are the evaluated thermal conductivities. Solid and dashed lines are the values calculated by the three porosity correction equations.

temperatures above 1673 K. The measurements were carried out at increasing temperatures in intervals of 100 K under a vacuum of less than 1×10^{-3} Pa. Thermal diffusivities were measured three times at each temperature and were averaged. A schematic diagram of the experimental set-up is given in Fig. 4.

The temperature response detected by the infrared detector was recorded as digital values into a personal computer. Thermal diffusivities were calculated from the recorded data by the curve-fitting method [16]. The increase of the specimen thickness during measurements was taken into consideration by using the equation reviewed by Carbajo et al. [2].

2.3. Thermal conductivity calculation

The thermal conductivity data were calculated from diffusivity measurements by the following equation:

$$\lambda(T) = a(T)\rho(T)C_p(T) \tag{1}$$

where $\alpha(T)$ is thermal diffusivity, $C_p(T)$ is the heat capacity at constant pressure and $\rho(T)$ is density of the specimen.

The density at temperature T was obtained by the equations reviewed by Carbajo et al. [2]. For the estimation on the heat capacity of $(U_{0.7-z}Pu_{0.3}Am_z)O_2$, the additive approximation according to Kopp's law was applied, $C_p = (0.7-z) \times C_p(UO_2) + 0.3 \times C_p(PuO_2) + z \times C_p(AmO_2)$, using the values of $C_p(UO_2)$ [2], $C_p(PuO_2)$ [2] and $C_p(AmO_2)$ [17].

3. Results and discussion

3.1. Influence of density

The thermal conductivities of 2%Am-MOX specimens of different porosities were measured. These results are shown in Fig. 5 as a function of porosity. The porosity p was defined conventionally from the theoretical density ρ_{th} and the real density ρ of a specimen as follows:

$$p = \frac{\rho_{th} - \rho}{\rho_{th}} = 1 - \left(\frac{\rho}{\rho_{th}}\right) \tag{2}$$

In order to derive the thermal conductivity λ_0 of a specimen of theoretical density from the thermal conductivity λ of a real specimen of porosity p, the experimental data were fitted with the following porosity correction equations given by Loeb [18], Maxwell and Eucken [19–21] and Schultz [22].

$$\begin{aligned} \lambda &= F \times \lambda_0 \\ F &= 1 - \alpha \times p, && \text{Loeb equation} \\ F &= (1-p)/(1+\beta \times p), && \text{Maxwell–Eucken equation} \\ F &= (1-p)^{\gamma}, && \text{Schultz equation} \end{aligned} \tag{3}$$

Here, F is the porosity correction factor and the values of α, β and γ are determined from the experimental values. From the results of fitting, the following values were obtained: $\alpha = 1.37$, $\beta = 0.52$ and $\gamma = 1.44$.

Previously, a technical team from IAEA [23], Biancheria [24] and Schultz [22] recommended $\alpha = 2.5 \pm 1.5$ for the Loeb equation, $\beta = 0.5$ for the Maxwell–Eucken equation, and $\gamma = 1.5$ for the Schultz equation. In the present study, $\beta = 0.5$ recommended by Biancheria agreed well with $\beta = 0.52$ which was determined from the experimental value. Thus, the Maxwell–Eucken correction factor with $\beta = 0.5$ was adopted for the following analysis.

3.2. Influence of Am-content

The measured data were corrected to the values at the theoretical density. The thermal conductivities of UO_2 and Am-MOX pellets are shown in Fig. 6 as a function of temperature together with conductivities of UO_2 reviewed by Carbajo et al. [2]. The data for UO_2 obtained in the present study and those of Carbajo et al. are in good agreement. Fig. 7 shows the thermal conductivities of Am-MOX pellets as a function of Am-content. The effect of Am addition of less than 3% on the thermal conductivity was slight at low temperatures (below 1200 K), but this effect was hardly to be observed at high temperatures (above 1200 K).

The thermal resistivities, the reciprocals of thermal conductivities, of Am-MOX increased linearly with temperature up to about 1500 K, which implies that the thermal conductivities of Am-MOX could be expressed by the following equation, based on the classical phonon transport model:

$$\lambda = (A + BT)^{-1} \tag{4}$$

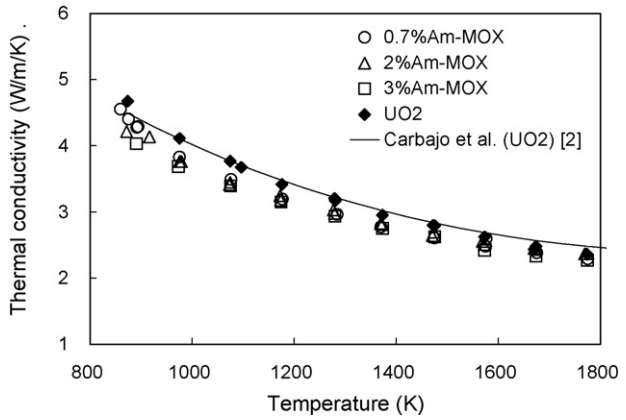

Fig. 6. Thermal conductivities of UO_2 and near-stoichiometric 0.7, 2 and 3%Am-MOX as a function of temperature. Open marks are the evaluated thermal conductivity results of Am-MOX, and solid marks are those of UO_2. The solid line is the values reviewed by Carbajo et al. [2].

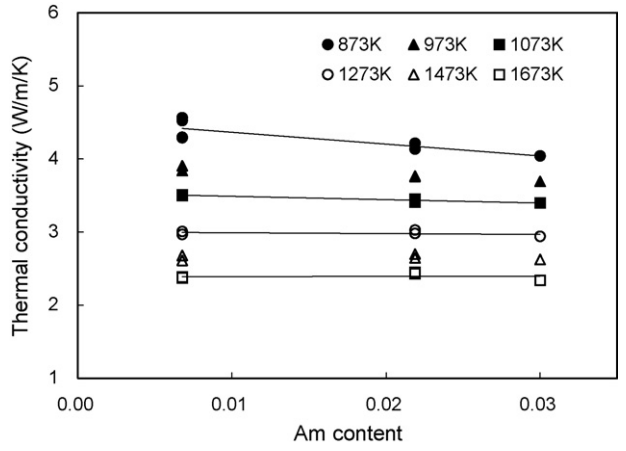

Fig. 7. Thermal conductivities of near-stoichiometric 0.7, 2 and 3%Am-MOX as a function of Am content. Open and solid marks are the thermal conductivity results evaluated at different temperatures.

The values of A and B were determined by fitting the thermal conductivity data to Eq. (4). They are shown in Table 3. The values of A increased linearly with an increase of Am-content, while those of B decreased slightly with increase of Am-content although the variation was small.

A corresponds to the thermal resistivity caused by the phonon-lattice defect interactions, or the lattice defect thermal resistivity.

BT corresponds to that caused by the phonon–phonon interactions based on Umklapp processes, or the intrinsic lattice thermal resistivity.

Table 3
Coefficients A and B obtained from the results of measurement

Specimen	A	B
0.7%Am-MOX	2.333×10^{-2}	2.434×10^{-4}
2%Am-MOX	2.727×10^{-2}	2.434×10^{-4}
3%Am-MOX	4.189×10^{-2}	2.336×10^{-4}

Based on Ambegaoker's theory [25], A is represented by the following relationship.

$$A = \frac{\pi^2 \overline{V} \theta}{3\overline{v}^2 h} \sum_i \Gamma_i \tag{5}$$

Here $\bar{V}$ is the average atomic volume, θ the Debye temperature, $\bar{v}$ the average phonon velocity, h the Planck's constant, and Γ_i is the scattering cross section parameter of phonons by point defect i and is approximately given by the following equation [26]:

$$\Gamma_i = X_i \left[\left(\frac{\bar{M} - M_i}{\bar{M}} \right)^2 + \varepsilon \left(\frac{\bar{r} - r_i}{\bar{r}} \right)^2 \right] \tag{6}$$

where X_i and M_i are the atomic fraction and the mass of point defect i, respectively, $\bar{M}$ is the average atomic mass of the host lattice site, r_i the atomic radius of the point defect i in its own lattice, $\bar{r}$ the average atomic radius of the host lattice site, and ε is the parameter representing the magnitude of lattice strain generated by the point defect. The parameter ε is obtained by fitting the experimental data to Eq. (6) [26]:

In an actinide oxide, uranium can occur as U^{4+}, U^{5+} and U^{6+}, plutonium as Pu^{3+} and Pu^{4+}, and americium as Am^{3+} and Am^{4+}. Thus, many kinds of combinations of cation valences can be considered in the mixed oxide (U, Pu, Am)O_2. However, U^{6+} is stable at low temperature where UO_3 exists, and americium becomes trivalent more easily than plutonium. From these reasons, two ionic structures (U^{4+}, U^{5+}, Pu^{4+}, Am^{3+})O_2 and (U^{4+}, Pu^{4+}, Am^{4+})O_2 were used in the investigation of point defect scattering.

First, the value A of Am-MOX was calculated in the ionic structure, ${U_{(0.7-2z)}}^{4+}$ ${U_z}^{5+}$ ${Pu_{0.3}}^{4+}$ ${Am_z}^{3+}$ ${O_2}^{2-}$. For the stoichiometric composition, the amount of O^{2-} ions in the anion sublattice is independent of the Am-content, and the four cations, U^{4+}, U^{5+}, Pu^{4+} and Am^{3+} ions can be considered as the phonon scattering centers, which contribute to the change of lattice defect thermal conductivity.

The sum $\sum \Gamma_i$ is expressed as follows:

$$\sum \Gamma_i = \Gamma_{U^{4+}} + \Gamma_{U^{5+}} + \Gamma_{Pu^{4+}} + \Gamma_{Am^{3+}} = \left(\frac{(X_{U^{4+}} + X_{U^{5+}}) M_U^2 + X_{Pu^{4+}} M_{Pu}^2 + X_{Am^{3+}} M_{Am}^2}{\overline{M}^2} - 1 \right)$$
$$+ \varepsilon \left(\frac{X_{U^{4+}} r_{U^{4+}}^2 + X_{U^{5+}} r_{U^{5+}}^2 + X_{Pu^{4+}} r_{Pu^{4+}}^2 + X_{Am^{3+}} r_{Am^{3+}}^2}{\bar{r}^2} - 1 \right) \tag{7}$$

where $\bar{M}$ is simply the average atomic mass and $\bar{r} = (0.7 - 2z)\, {r_U}^{4+} + z {r_U}^{5+} + 0.3\, {r_{Pu}}^{4+} + z {r_{Am}}^{3+}$.

The quantities needed to evaluate A were accessible except for the Debye temperature and the average phonon velocity.

The Debye temperature can be estimated by Eq. (8) according to the Lindemann relationship [27] as follows:

$$\theta = C\frac{(T_M)^{1/2}}{(\bar{M})^{1/2}(\bar{V})^{1/3}} \quad (8)$$

where T_M is the melting temperature. Assuming that the constant C of Am-MOX is the same as that of UO_2, the Debye temperature of Am-MOX is obtained by the following equation:

$$\frac{\theta_{AmMOX}}{\theta_{UO_2}} = \frac{(\overline{M_{UO_2}})^{1/2}(\overline{V_{UO_2}})^{1/3}(T_{M\text{-}AmMOX})^{1/2}}{(\overline{M_{AmMOX}})^{1/2}(\overline{V_{AmMOX}})^{1/3}(T_{M\text{-}UO_2})^{1/2}} \quad (9)$$

where $T_{M\text{-}UO_2}$ and $T_{M\text{-}AmMOX}$ are melting temperatures of UO_2 and Am-MOX, respectively.

In this estimation, we used the value of $\theta_{UO_2} = 242$ K reported by Willis [28] and $T_{M\text{-}UO_2} = 3138$ K as measured by Latta and Fryxel [29]. The melting temperature of Am-MOX, $T_{M\text{-}AmMOX}$, was estimated from the melting temperatures and the heats of fusion of UO_2 [29,30], PuO_2 [31,32] and AmO_2 [33,32] by using the ideal solution model.

The average phonon velocity can be estimated by the following Eq. (10) derived from the Debye approximation.

$$\bar{v}_{AmMOX} = \bar{v}_{UO_2}\left(\frac{\theta_{AmMOX}}{\theta_{UO_2}}\right)\left(\frac{a_{AmMOX}}{a_{UO_2}}\right) \quad (10)$$

For Am-MOX, the value of A was estimated by using Eqs. (5)–(10). The parameter $\varepsilon = 44$ was obtained by fitting the present experimental data. This value was not so different from the $\varepsilon = 55 \pm 50$ reported for (U, Pu)O_2 by Fukushima et al. [4].

Similar calculations and fittings were done to determine the values of A in the ionic structure, $(U^{4+}, Pu^{4+}, Am^{4+})O_2$. Fig. 8(a) shows the experimental and calculated values of A as a function of Am-content. The thermal conductivity of MOX fuel containing a few percent of Am was found to be well represented, if the ionic structure of Am-MOX was assumed to be $U_{(0.7-2z)}{}^{4+}U_z{}^{5+}Pu_{0.3}{}^{4+}Am_z{}^{3+}O_2{}^{2-}$.

B is represented by the following relationship [34]:

$$BT = \frac{\gamma^2 T}{\left[\frac{24}{10}4^{1/3}\left(\frac{h}{k}\right)^3 \bar{M}\bar{V}^{1/3}\theta^3\right]} \quad (11)$$

where γ is the Grüneisen constant and k is the Boltzmann constant.

For Am-MOX, the value of B was estimated by assuming that the γ value of Am-MOX was the same as that of UO_2.

$$\frac{B_{AmMOX}}{B_{UO_2}} = \left(\frac{m_{AmMOX}}{m_{MOX}}\right)^{1/2}\left(\frac{a_{AmMOX}}{a_{MOX}}\right)^2\left(\frac{T_{M\text{-}MOX}}{T_{M\text{-}AmMOX}}\right)^{3/2} \quad (12)$$

The value of B in UO_2 was that of Gibby [3]. Fig. 8(b) compares B obtained by fitting experimental data and the one calculated by Eq. (12). It was found that B obtained from experimental data was represented well by Eq. (12) thus the Am-content had little effect on the B value. Fig. 9 compares the thermal conductivity obtained from the experiment and that calculated using the values of A and B derived from Eqs. (5)–(12).

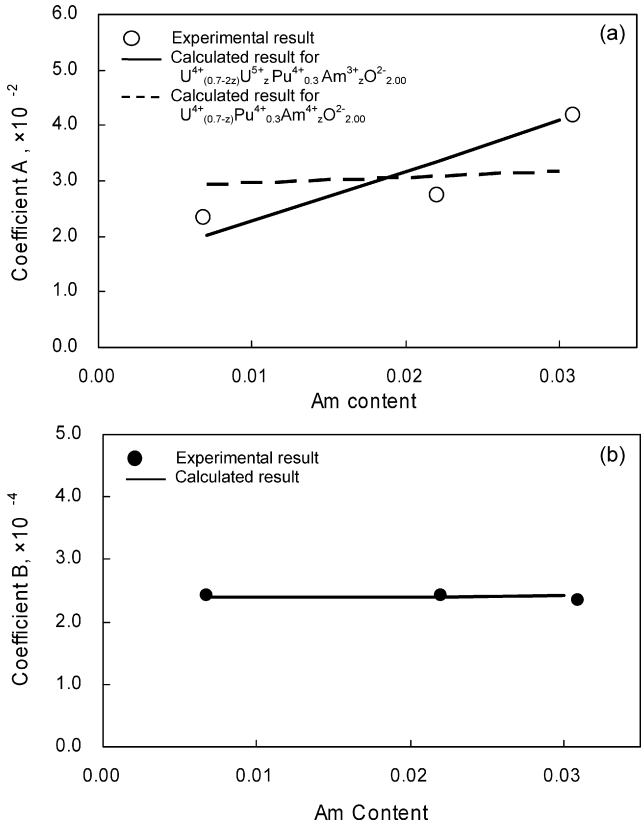

Fig. 8. Coefficients A and B as a function of Am content in Am-MOX. (a) Open marks are the values of A deduced from the experimental data. The solid and dashed lines show the calculated values of A. (b) Solid marks are the values of B deduced from the experimental data. The solid line shows the calculated values of B.

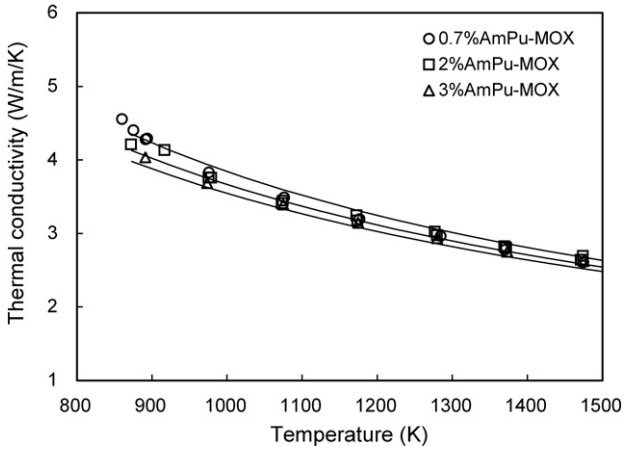

Fig. 9. Comparison between the experimental and calculated thermal conductivities. Open marks are the thermal conductivities evaluated from the experimental data. Solid lines are the thermal conductivities calculated from the phonon scattering model.

4. Conclusions

The thermal conductivities of $(U_{0.7-z}Pu_{0.3}Am_z)O_2$ solid solutions ($z = 0.007$–0.03) were studied by the laser flash method in the temperature range from 900 to 1773 K. These results are summarized as follows:

(1) The dependence of thermal conductivities on the effective porosity could be represented by the Maxwell–Eucken equation with the correction coefficient β of 0.5.
(2) The thermal conductivities of MOX fuels containing a few percent of Am decreased slightly with increasing Am-content. The thermal conductivities up to about 1500 K satisfied the classical phonon transport model, $\lambda_0 = (A + BT)^{-1}$. The coefficient A increased linearly, but the coefficient B hardly varied with an increase of the Am-content.
(3) The coefficients A and B obtained in the experiment were found to be theoretically well explained, assuming that the chemical formula of Am-MOX was $U_{(0.7-2z)}{}^{4+}U_z{}^{5+}Pu_{0.3}{}^{4+}Am_z{}^{3+}O_2{}^{2-}$. The coefficient A could be approximated by the simple linear relationship. The coefficient B was assumed to be constant. The following relations were found to be fulfilled:

$$\lambda_0 = \frac{1}{A + BT}$$

$$A = 0.90 \times z + 0.014\,(\mathrm{mK/W}),$$

$$B = 2.40 \times 10^{-4}\,(\mathrm{m/W})$$

Acknowledgements

The authors acknowledge the collaboration of Messers. H. Uno, S. Shinohara, M. Shinada, M. Kowata, T. Tamura, H. Sugata, T. Sunaoshi, M. Kuwana, K. Shibata and H. Sato in sample preparation and analyses. Special thanks are also given to Professor Emeritus of Kyushu University, Dr. H. Furuya for valuable discussions.

References

[1] D.G. Martin, J. Nucl. Mater. 110 (1982) 73.
[2] J.J. Carbajo, G.L. Yoder, S.G. Popov, V.K. Ivanov, J. Nucl. Mater. 299 (2001) 181.
[3] R.L. Gibby, J. Nucl. Mater. 38 (1971) 163.
[4] S. Fukushima, T. Ohmichi, A. Maeda, M. Handa, J. Nucl. Mater. 116 (1983) 287.
[5] A.B.G. Washington, UK Atomic Energy Authority, TRGR-2236, September 1973.
[6] J.H. Harding, D.G. Martin, J. Nucl. Mater. 166 (1989) 223.
[7] Y. Philipponneau, J. Nucl. Mater. 188 (1992) 194.
[8] P.G. Lucuta, H.I. Matzke, I.J. Hastings, J. Nucl. Mater. 232 (1996) 166.
[9] W. Wiesenack, Proceedings of the ANS International Topical Meeting on LWR Fuel Performance, Portland, OR, 1997, p. 507.
[10] K. Ohira, N. Itagaki, Proceedings of the ANS International Topical Meeting on LWR Fuel Performance, Portland, OR, 1997, p. 541.
[11] C.R. Ronchi, J. Appl. Phys. 85 (1999) 776.
[12] C. Duriez, J.P. Alessandri, T. Gervais, Y. Philipponneau, J. Nucl. Mater. 277 (2000) 143.
[13] M. Kato, T. Tamura, K. Konashi, S. Aono, J. Nucl. Mater. 344 (2005) 235.
[14] K. Morimoto, M. Kato, U. Uno, A. Hanari, T. Tamura, H. Sugata, T. Sunaoshi, S. Kono, J. Phys. Chem. Solids 66 (2005) 634.
[15] M. Kato, H. Uno, T. Tamura, K. Konashi, Y. Kihara, Proceedings of the Eighth Actinide Conference, Actinides 2005, Manchester, UK, 2005, p. 367.
[16] T. Baba, A. Cezairliyan, Int. J. Thermophys. 15 (1994) 343.
[17] E.H.P. Cordfunke, R.J.M. Konings, Thermochemical Data for Reactor Materials and Fission Products, North-Holland, 1990.
[18] A.L. Loeb, J. Am. Ceram. Soc. 37 (1954) 96.
[19] J.C. Maxwell, Treatise on Electricity and Magnetism, vol. 1, 3rd ed. Oxford University Press (1891), reprinted by Dover, New York (1954).
[20] A. Eucken, Forsch. Gebiete Ingenieurw. B3, Forschungsheft No. 353 (1932) 16.
[21] H. Fricke, Phys. Rev. 24 (1924) 575.
[22] B. Schultz, High Temp. High Pressure 13 (1981) 649.
[23] Report of the Panel on Thermal Conductivity of Uranium Dioxide held in Vienna in 1965, Technical Reports Series No.59, IAEA, Vienna, 1966.
[24] A. Biancheria, Trans. Am. Nucl. Soc. 9 (1966) 15.
[25] V. Ambegaoker, Phys. Rev. 114 (1959) 488.
[26] B. Abeles, Phys. Rev. 131 (1963) 1906.
[27] F.A. Lindemann, Phys. Z 11 (1910) 609.
[28] B.T.M. Willis, Proc. Roy. Soc. (London) A274 (1963) 134.
[29] R.E. Latta, R.E. Fryxel, J. Nucl. Mater. 35 (1970) 195.
[30] J.K. Fink, J. Nucl. Mater. 279 (2000) 1.
[31] W.L. Lyon, W.E. Baily, J. Nucl. Mater. 22 (1967) 332.
[32] L.F. Epstain, J. Nucl. Mater. 22 (1967) 340.
[33] R.E. McHenry, Trans. Am. Nucl. Soc. 8 (1965) 75.
[34] G. Leibfried, E. Schlamann, Akad. Wiss. Gottingen, Math. Physik. KI II-A (1954) 71.